

FlatFitFab: Interactive Modeling with Planar Sections

James McCrae
University of Toronto
mccrae@dgp.toronto.edu

Nobuyuki Umetani
University of Tokyo
n.umetani@gmail.com

Karan Singh
University of Toronto
karan@dgp.toronto.edu

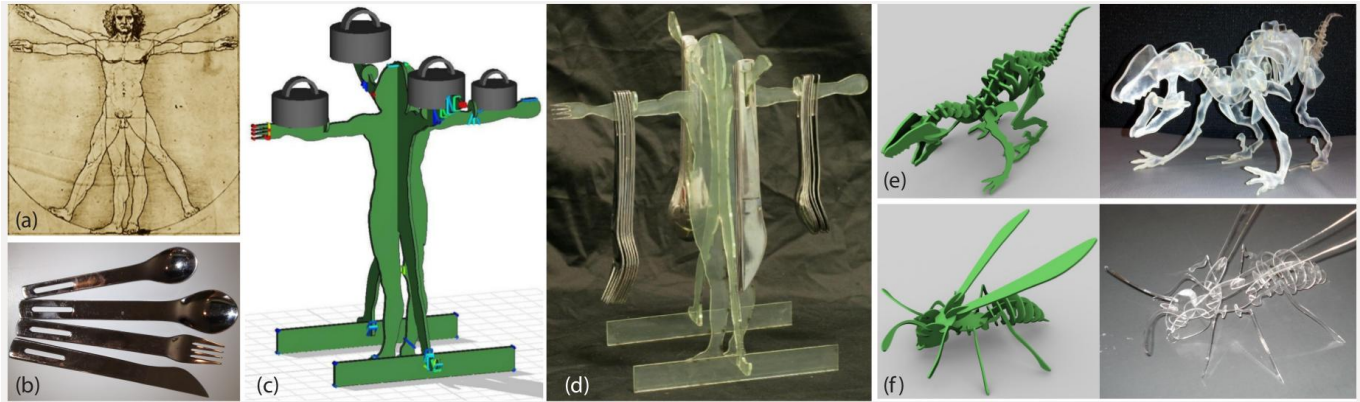


Figure 1. FlatFitFab is a comprehensive system for the interactive modeling, simulation and fabrication of planar section assemblies: Inspirational 3D models or images (the Vitruvian man) (a), and physical object parameters (cutlery weight and dimension) (b), feed into the interactive creation and composition of 3D planar sections (c) using a novel single-stroke workflow. Stress along planar sections (red and blue lines), subject to gravity and external forces (cutlery weight), is interactively simulated and visualized (c). Instant feedback on geometric stability, assembly and connectedness, further ensures that fabricated sections perform their intended function, e.g. a cutlery holder (d). A novel vocabulary of procedural operations designed for intersecting planar sections, e.g. vertebrae along the dinosaur spine (e), enables rapid and complex modeling by both experts (e) and amateurs (f).

ABSTRACT

We present a comprehensive system to author planar section structures, common in art and engineering. A study on how planar section assemblies are imagined and drawn guide our design principles: planar sections are best drawn in-situ, with little foreshortening, orthogonal to intersecting planar sections, exhibiting regularities between planes and contours. We capture these principles with a novel drawing workflow where a single fluid user stroke specifies a 3D plane and its contour in relation to existing planar sections. Regularity is supported by defining a vocabulary of procedural operations for intersecting planar sections. We exploit planar structure properties to provide real-time visual feedback on physically simulated stresses, and geometric verification that the structure is stable, connected and can be assembled. This feedback is validated by real-world fabrication and testing. As evaluation, we report on over 50 subjects who all used our system with minimal instruction to create unique models.

ACM Classification Keywords

H.5.2. User Interfaces: Graphical user interfaces; I.3.5 Computational Geometry and Object Modeling: Curve, surface, solid, and object representations.

Permission to make digital or hard copies of all or part of this work for personal or classroom use is granted without fee provided that copies are not made or distributed for profit or commercial advantage and that copies bear this notice and the full citation on the first page. Copyrights for components of this work owned by others than ACM must be honored. Abstracting with credit is permitted. To copy otherwise, or republish, to post on servers or to redistribute to lists, requires prior specific permission and/or a fee. Request permissions from permissions@acm.org.
UIST '14, October 05–08 2014, Honolulu, HI, USA.
Copyright © 2014 ACM 978-1-4503-3069-5/14/10...\$15.00.
<http://dx.doi.org/10.1145/2642918.2647388>

Author Keywords

Interaction; fabrication; shape modeling; planar sections.

INTRODUCTION

Artists and sculptors effectively use minimal representations of shape to tease and inspire human perception. Planar section assemblies have been used for more than a century by artists such as Calder and Picasso to express both realistic forms and abstract ideas (Figure 2 (top row)). Such abstractions can be fabricated economically using a variety of machines and materials to create architectural forms, functional furnishings and decorative art (Figure 2 (bottom row)). The increasing popularity of 3D modeling software and digital manufacturing devices, aimed at hobbyists, has fueled a flurry of recent research on amalgamating stages of design and manufacturing. 3D planar section assemblies, compactly manufactured and packed as 2D sheets, form a unique junction of design, manufacturing and human perception (Figure 1).

While the creation of manufacturable planar sections by slicing existing 3D objects (Figure 3 (right)) has received much attention in both research and industry (Autodesk 123D Make), artistic planar section structures rarely conform precisely to 3D models (Figure 3 (left, middle)). In fact, nearly all the structures shown in this paper cannot be created by simply slicing a 3D object using planes. In practice, like architecture [17], planar section assemblies are inspired by a mix of 2D images, 3D models, physical constraints and pure imagination. Fluid interfaces for creating such structures from scratch using a mixed bag of design inspirations, are relatively unexplored. We present such an interface, that



Figure 2. Outdoor planar section sculptures ©Alexander Calder (top row) . Planar section use (bottom row) in architecture (left), home furnishings (centre) and interior decoration (right).

incorporates images, 3D models and constraints into a single homogeneous workflow, to create intricate and physically sound planar section assemblies. Our system is a judicious combination of many novel and existing components, bigger than the sum of its parts and applicable to broader areas 3D modeling, deformation and scaffolding (for sketching [22] or animatronics [15, 31]). Specifically, the single stroke drawing workflow and magnetic cut deformation of 3D models are entirely novel components, and the overall physical simulation and correlated affine operations (the rib cage in Figure 9) are novel in the context of planar section structures.

Following a survey of *related work*, we present an *exploratory study* into planar section drawing. Conclusions from the study, and the simple observation that a planar section has one dimension less than a 3D model, motivate the design of our *interactive interface*, vocabulary of *procedural operations*, real-time *physical simulation* and *fabrication* constraints. As *evaluation*, we present the results of real-world fabrication and testing, and report on the usage of our system by over 50 high-school students and other users.



Figure 3. Planar sections can represent non-manifold scaffolds (left), conform partly (middle), or entirely (right) to 3D object contours.

RELATED WORK

Our system is informed by prior work on 3D shape abstraction, physical simulation, fabrication and interactive design.

3D shape abstraction for conceptual design: Much of sketch-based conceptual design [2, 22, 24] draws inspiration from traditional design drawing [5], to build sparse 3D curve representations of shape. A large percentage of these curves such as design cross-sections [24], are in fact planar and drawn to perceptually convey 3D shape. The planar contours created by our system are often logical completions of

such design cross-sections. Planar contours drawn in 2D are fundamental to modeling systems from the seminal Sketchpad [25] to Teddy [8] and its successors [19]. Our single-stroke contour drawing workflow can streamline curve creation in these systems. Planar symmetry is also intrinsic to 3D shape and extensively used in interactive interfaces, both to infer and replicate 3D shape across symmetry planes [2], and such planar symmetry hierarchies can be readily authored using our system. The fact that most 3D objects can be satisfactorily abstracted by humans using a small number of planar sections [12], is a testament to the expressive power of planar section assemblies.

Physical simulation and analysis: Feedback on geometric constraints and physical simulation during interactive 3D modeling creates functionally improved models and reduces wasted iterations of real fabrication and testing [18, 27]. As general structural simulation using the Finite Element Method is still too slow for real-time feedback, reduced or approximate physical models for specific design problems have been developed. For example, interactive physical analysis has been shown to aid users in furniture design [27], to guide forms toward structurally sound masonry buildings [29], or to geometrically adapt 3D sculptures to stand once fabricated [18]. We similarly, propound a novel physics model based on cross-section samples [28], to compute stresses within and between connected planar sections in real-time.

Shape fabrication: A large body of recent research addresses problems on design and processing of 3D shapes for fabrication, by 3D printers [18], or using 2D routers such as laser cutters to create planar [9] or even LaserOrigami [13] bent sections, with a variety of joints and flexures [1]. Most work on planar sections is focused on automated processing of assemblies created by slicing existing 3D objects [4, 7, 12] (Figure 3 (right)), and formalizing geometric constraints necessary for the assembly of connected 3D planar sections [23]. We instead focus on the interactive creation of general planar section assemblies (a superset of sliced 3D models), combining elements of interaction, procedural modeling, geometric analysis and real-time simulation to produce structures that are both physically functional and aesthetically pleasing.

Interactive design: Within the interactive design space, planar sections have been used to make V-style pop-ups [11], or radial section lampshades by sketching volumes in 3D [30]. Planar sections have also been used in furniture design from rectilinear shapes [16] or extruded profiles [20], created using 2D interfaces, with regularity constraints [9]. We in contrast, enable planar section assembly creation in-situ, using procedural operations to facilitate regularity and complexity.

PLANAR SECTION EXPLORATORY STUDY

We performed an exploratory study to understand how users imagine and draw planar sections in 3D. We asked 6 users with varying artistic capability and 3D modelling experience to create planar section representations of both imagined objects and a set of reference 3D models (Figure 4). We developed an interactive system for this study that allowed planar curve sketching in 3D on a user manipulated planar canvas.

The system also logged user interaction details: strokes, canvas manipulation, camera motion and other geometric measurements. We analyzed the creations, log data and interviewed users to conclude the following design principles:

Design collateral: Users remarked that while their creations were often inspired by 2D images or 3D objects, the planar section assemblies they imagined would only partially conform to input boundaries, and connect expressively in the interior. Our proposed system allows users to meaningfully combine images, 3D models and blank canvas creation within a single modelless drawing workflow.

Plane orthogonality and regularity: We found drawing planes to be predominantly parallel or perpendicular to each another. Intersecting planes almost always met orthogonally. We also observed shape regularities between planar section contours, reflecting the connection between planes and symmetry in design [5]. We capture these regularities by procedural operations. Further, most cutting devices operate orthogonal to the planar contour, requiring intersecting sections to fit together orthogonally. We enforce and exploit this orthogonality property in our proposed interface.

Frontoparallel views: Sketching error, even for experts drawing on 3D planes, is clearly correlated to the degree of foreshortening of the plane [21]. We thus use frontoparallel views by default when drawing contours, since our own analysis confirmed that artists naturally tended to sketch from or near frontoparallel views, and sketching curves on oblique 3D planes consistently produced unpredictable results.

Single-view interface: We also experimented with a multi-view system such as [9], where users worked in disparate viewports to manipulate planes and contours. Artists overwhelmingly preferred a single 3D view for multiple reasons: maximal use of screen space, attention and drawing cursor is not shifted between views, and a single view provides a modeling context between new curves and the evolving design.

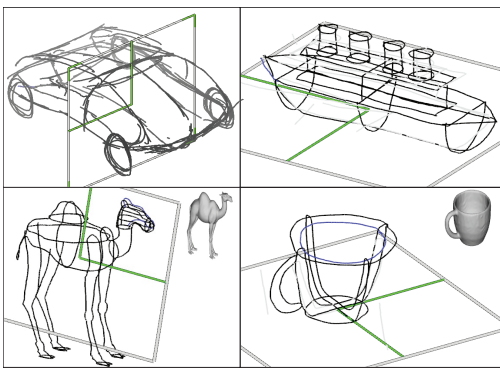


Figure 4. Pilot study artist creations: freeform objects (top row); reference objects with object shown inset (bottom row).

CREATING PLANAR SECTIONS

Our interface allows a mix of sketch-based drawing and CAD style control point editing of shape contours. Planar section structures may be exported in-situ in 3D (OBJ for visualization) or 2D (SVG for fabrication).

Single stroke planar section creation.

Central to our approach is the creation of a new planar section, accomplished using a single stroke, illustrated in Figure 5 and the accompanying video. This stroke entails:

Defining the slit: The stroke first defines the *slit*, where two orthogonal planar sections join. The stroke starts on the interior of an existing planar section, defining one endpoint for the slit axis, and defines a slit when the cursor exits the planar section interior. A new canvas plane containing the slit is defined orthogonal to the existing planar section.

View rotation and translation: The system rotates the view so the new canvas plane is viewed frontoparallel. Importantly, rotation is constrained so the slit endpoint remains fixed beneath the cursor. This rotation preserves drawing focus and view translation is used to ensure there is available screen space to draw the next planar section contour.

Deadzone: Using an earlier prototype, artists felt constrained being forced to start the planar section contour at the slit endpoint. The *deadzone*, a capsule shaped region in the viewport around the slit, addresses this issue. The deadzone prevents the planar section contour from being defined until the cursor exits the region, which has a fixed radius relative to the dimensions of the viewport. A planar section contour can thus begin near either slit endpoint, or anywhere in between.

Contour sketching: As the user sketches, our system fits a cubic Bézier spline, with a final Bézier segment to close the curve. When the stroke is completed, the planar section is created, completing the interaction. When there are no existing planar sections to start with, the contour is defined on a frontoparallel viewed plane that intersects a point at a fixed distance above the origin (default: 3.3 units).

A stroke principally on one side of the slit axis is effectively used to indicate symmetry across a planar section. If the ratio of maximal distances of the stroke on either side of the axis is sufficiently high (6.0 in our implementation), the stroke is mirrored across the axis and smoothly joined (Figure 6).



Figure 6. A planar section contour drawn principally on one side of the slit (left), is mirrored across slit and smoothly joined (right).

Template 3D objects

We typically use watertight 3D mesh templates, that produce closed planar section contours, but can also handle arbitrary meshes by smoothly joining open contours using cubic Bézier segments. The model is scaled (10 units) and centered in our interface to rest upon the ground plane (minimum Y vertex set to $Y = 0$). Precise ground contact is not essential as the planar sections are free to deviate from the template and are clipped to ensure proper ground contact. The model is rendered transparently so as not to obscure the planar sections

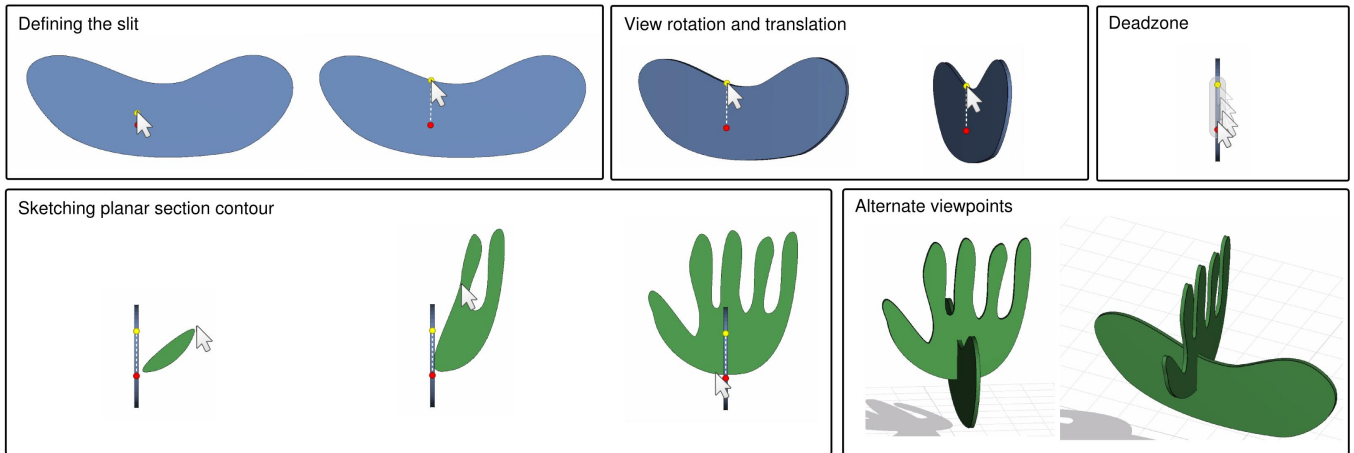


Figure 5. Single stroke planar section creation: once the user defines the slit connecting a new planar section to an existing section, the system rotates around the slit endpoint to a frontoparallel view (top row); the user moves outside the deadzone (top right) to begin sketching the contour (bottom row).

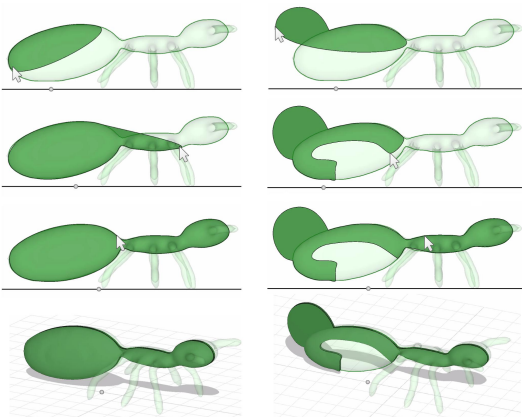


Figure 7. Snapping to a template object: a user sketches roughly along the guide curve to snap to the template object (left column) or deviate from it when desired (right column).

and serves as a guide for planar section creation ($\alpha = 0.25$ with back-face culling enabled in our implementation).

Ideal templates: Once the user draws the slit to define a new plane, guide curve(s) that are the intersection of plane and the template are shown. The user can then simply snap to desired parts of guide curves by over-tracing (distance to curve 0.5 units by default) or smoothly deviate from them (Figure 7).

Non-ideal templates: Objects with large articulations or highly non-planar curvature lines are inherently ill-suited to planar sections. Artists locally distort nearby surface features of such shapes so they lie on planar section contours. We propose a *magnetic cut* spatial deformation, that captures this behaviour. Points P within a distance r to the plane are attracted along the plane’s normal N , towards the plane (Figure 8) to $P' = P + N [N \cdot (Q - P) + (N_P \cdot N)r]$, where Q is a point on the plane and N_P is the surface normal at P . The deformation moves the local shape silhouette viewed along N to lie along the planar section contour. In practice this works well for small deformations, and large articulations are best handled piece-wise, using multiple planar sections.

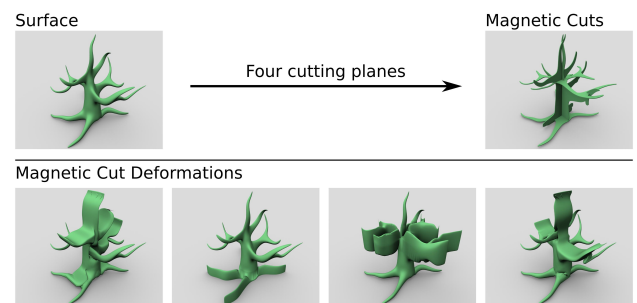


Figure 8. The template (top left) and 4 magnetic cut planar sections (top right). The deformation relative to each plane is shown (bottom row).

PROCEDURAL MODELLING

We are inspired by procedural modelling research [6, 10, 14], in defining a vocabulary of modeling operations that provide specific support for various inter-plane and contour shape regularities observed in artistic planar section structures.

Affine operations

We define a family of affinely transformed replicas of a *clone* planar section along a *root* planar section. The basic operation clones a planar section along one side of the root planar section, preserving the normal direction of the clone at a fixed offset. The replicated sections are also translated along the intersection axis, to ensure that the line of intersection between replica and root is of equal length for all replicas (Figure 9). Alternatively, sections can be replicated to conform to the root contour, by rotating the replicas using the tangent direction along the root. To keep the orientation of replicas consistent, the relative angle between the clone plane normal and root boundary tangent is maintained across all revolved replicas (Figure 11). We observe that often the scale of replicas naturally varies with the local thickness of the root contour, for example the ribs are larger where the spine is thicker and vice-versa (Figure 9). We can support this behaviour by uniformly scaling replicas based on local thickness of the root contour, computed as the contour girth along the line of intersection between replica and root (Figures 9 and 10).

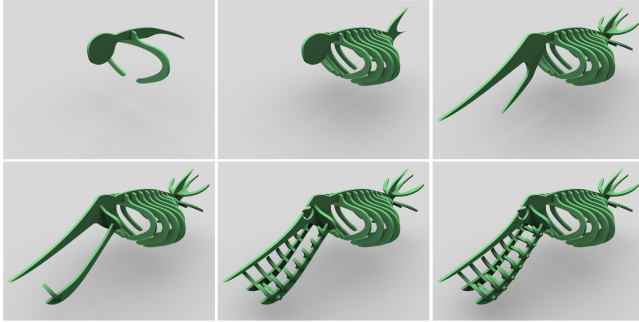


Figure 9. Fish skeleton created using affine operations, showing a variation in rib and tooth size with the local thickness of the spine and jaw.

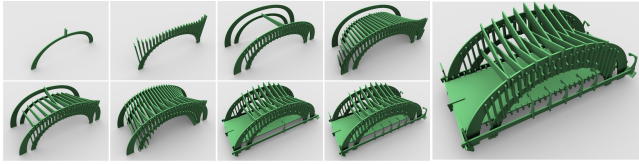


Figure 10. A bridge created using the range of affine operations.

Blend operation

The blend operation creates blended copies of two cloned planar sections P and Q along a root planar section, as simultaneously interpolated 2D contours and affinely transformed 3D planes, (Figure 12). We morph 2D contours by first finding a point-point correspondence between contours P and Q and then simply interpolate corresponding 2D point positions. The correspondence is computed by uniformly sampling both contours using n points (indexed p_i, q_i) and then finding an offset k that minimizes the sum of pairwise distances between points in P and Q (including a reversed point order), $\min_{k \in \{0, \dots, n-1\}} \sum_{i=0}^{n-1} \|p_{((k+i) \bmod n)} - q_i\|_2$. The interpolated contours are then replicated in 3D, using an affine operation, where the relative angle between the clone plane normal and root tangent at P and Q is also interpolated.

Branching operation

The re-configurable nature of procedural planar sections also lends itself to hierarchical modeling. Given a planar section

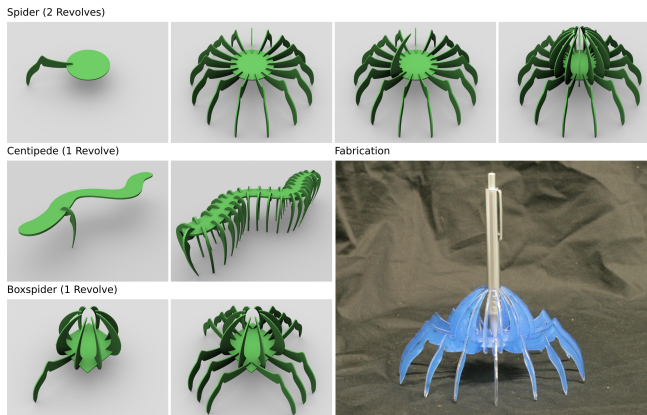


Figure 11. A number of insect-like examples, created using affine revolve operations. A fabricated spider holds a pen (bottom right).

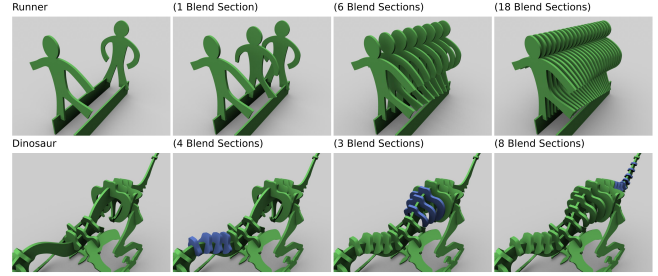


Figure 12. A figure in two different poses is blended using 1, 6 or 18 planar sections (top row). Three blend operations (rendered in blue) are used to create vertebrae and ribs along the dinosaur spine (bottom row).

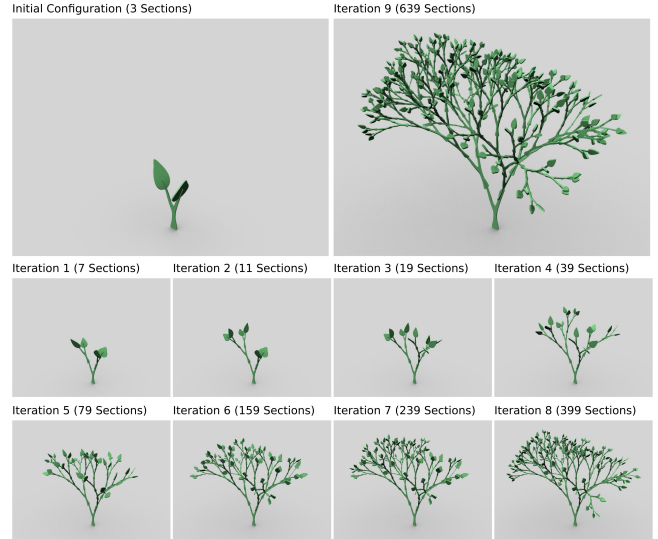


Figure 13. A Y-shaped root section and two leaf-shaped child sections (top left), produce a planar section tree structure (top right) after 9 iterations of branch operations (bottom rows).

structure with a designated *root* section, connected to *child* sections, a branch operation replaces one or more of the children with replicas of the entire hierarchy. The slit on the root section where the replicated hierarchy is attached is interactively specified by the user. The children to be replicated and the scale of the replicated hierarchy can be randomized or user-controlled to rapidly produce complex and natural-looking planar section hierarchies (Figure 13).

Grid operation

The physical dimensions of each planar section can be restricted by the size of the cutter-bed or material sheets used for fabrication. We address this using a grid operation that divides large sections into a collection of smaller sections

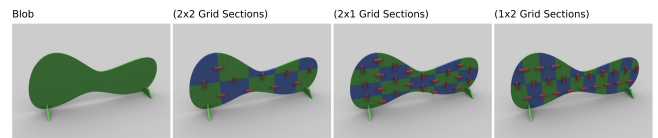


Figure 14. A planar section (left) is split into gridded sections (rendered in blue and green). H-shaped connecting sections (rendered in red) are automatically generated along grid edges.

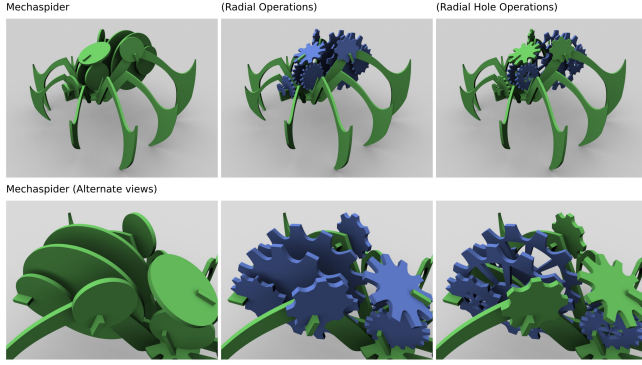


Figure 15. Radial operations are used to control planar section contours, producing the discs, gears (top row) and holes (bottom row) shown in blue.

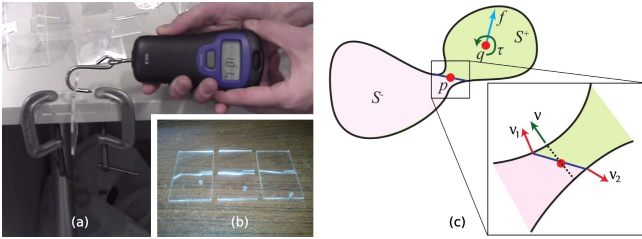


Figure 16. Experiment where force required for fracture was measured along three major axes on planar section joints (a). Fracture occurred in a consistent pattern, across planar sections (b). Visualization of our cross-sectional structural analysis, based on beam theory (c).

which assemble together using automatically generated H-shaped connectors (Figure 14). Such an operation can also be used to create decorative jigsaw puzzle-like tiled sections.

Radial contour operation

As an example of procedural control over the contour shape of planar sections, we allow users to control the radial profile of a section to make circles, stars, holes or gear shapes with varying holes and teeth (Figure 15).

PHYSICAL SIMULATION

Our system is designed to produce functional objects from planar sections that friction fit together along slits, such as the cutlery holder in Figure 1 or glass holders in Figure 17. Users convey functional use in our system by interactively placing external weights at various points on the planar section assemblies (Figure 1c, 17). We exploit the structure of planar section assemblies to formulate a novel physical model that is able to conservatively compute stresses across planar sections in real-time, using a combination of *inter-plane* and *intra-plane* analysis, with the computation of cross-sectional bending moments for a planar section structure.

Inter-plane Analysis

We assume planar sections to be undeformable and unbreakable rigid bodies, across which we compute forces on slit joints and contact points. Planar sections, subject to forces from external loads, joints, ground contact points, and internal gravitational force, are analyzed in static equilibrium. Planes rotate and translate in response to gravity and placed

weights and this movement is countered by computing contact and joint constraint forces to maintain the stability of the structure [27]. After the contact and joint forces have been computed, we analyze the stress within each planar section based on these forces.

Formally, a point $\mathbf{p} \in \mathbb{R}^3$ on a rigid planar section is moved as $\hat{\mathbf{p}}(\mathbf{R}, \mathbf{u}) = \mathbf{R}(\mathbf{p} - \mathbf{p}_{cg}) + \mathbf{p}_{cg} + \mathbf{u}$, where $\mathbf{p}_{cg} \in \mathbb{R}^3$ is the center of gravity of the section, $\mathbf{u} \in \mathbb{R}^3$ is the translation and $\mathbf{R} \in SO(3)$ is the rotation matrix. The translation and rotation for each section is obtained by energy minimization subject to joint constraints. The total energy of the rigid section structure is computed as the sum of potential energy as:

$$E = - \sum_{i \in S} mg \cdot \mathbf{u}^i - \sum_{i \in F} \mathbf{d}_i^w \cdot \mathbf{f}_i^w, \quad (1)$$

where S is the set of planar sections, F is the set of weights, \mathbf{d}^w is the displacement of the weight as a result of the sections' movement, and \mathbf{f}^w is the force from the weight. At each joint, we apply a joint constraint that prohibits the relative displacement and rotation of connected sections. Let two rigid sections A and B be connected at a joint point \mathbf{p}_J at the inner end of the slit. The joint point on section A for example after movement is $\mathbf{R}_A(\mathbf{p}_J - \mathbf{p}_{cg}) + \mathbf{p}_{cg} + \mathbf{u}_A$. The relative displacement constraint $(\mathbf{R}_A(\mathbf{p}_J - \mathbf{p}_{cg}) + \mathbf{p}_{cg} + \mathbf{u}_A) - (\mathbf{R}_B(\mathbf{p}_J - \mathbf{p}_{cg}) + \mathbf{p}_{cg} + \mathbf{u}_B) = 0$ thus implies that sections A and B remain connected at the joint point. A rotation constraint keeps the rotation of connected sections A and B the same, i.e. $(\mathbf{R}_A \mathbf{R}_B^T) = \mathbf{I}$. Contact constraints keep the distance of points of contact from the ground plane at zero. We minimize the total energy in Equation 1, subject to the displacement, rotation and contact constraints, using Newton's method, and obtain the constraint forces at joint and ground contact points (detailed in [27]).

Intra-plane Analysis

Our intra-plane analysis uses the joint and contact forces from inter-plane analysis to compute the bending moment acting on cross-sections of a plane [28] and its consequent stress using beam theory [26]. The forces at contact points on either side of a planar cross-section (we assume the section is not an annulus) induce bending moments that are equal and opposite in equilibrium (Figure 16c). Classifying the sidedness of contact points relative to the cross-section of a plane is straightforward, allowing us to compute bending moments efficiently. In beam theory, the ratio between bending moment and stress along a cross-section is called the *section modulus*. The section modulus in turn is proportional to the rectangular dimensions of the cross-section, implying that the narrower the cross-section, the greater the stress. In our implementation, we display weak cross-sections, where the stress exceeds $1/5$ the maximum stress the material can handle, color coded from blue to red for 20%-100% of the maximum stress.

Formally, let the force points (joint, contact and weight) be \mathbf{q}^i with linear force \mathbf{f}^i and torque τ^i (torque at contact points is zero), for $i \in K$, where K is the set of force points on a section (Figure 16c). In equilibrium, the linear forces sum to zero: $mg + \sum_{i \in K} \mathbf{f}^i = 0$ where m is the mass of the section.

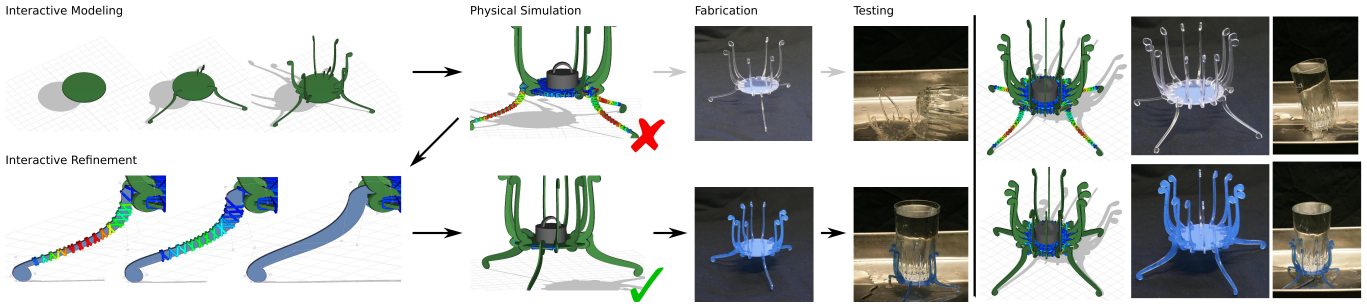


Figure 17. Our real-time physical simulation, interactively visualizes cross-sectional lines of stress along planar sections where fracture is likely (20%-100% maximum allowed stress rendered blue to red). Users interactively edit the model to satisfy both form and function. Physical fabrication of weak (top row) and strong (bottom row) variants of 3-legged (left) and 4-legged (right) glass holders validates predictions of fracture made by our system.

Moment equilibrium similarly, implies that the moment at the given point in the section \mathbf{p} becomes zero:

$$m\mathbf{g} \times (\mathbf{p}_{cg} - \mathbf{p}) + \sum_{i \in K} \mathbf{f}^i \times (\mathbf{q}^i - \mathbf{p}) + \boldsymbol{\tau}^i = 0. \quad (2)$$

We compute the bending moment at the center of a cross-section \mathbf{p} by partitioning Equation 2 into moments $\boldsymbol{\tau}^+$, $\boldsymbol{\tau}^-$ on either side of the cross-section S^+ and S^- (Figure 16c). $\boldsymbol{\tau}^+(\mathbf{p}) = m^+ \mathbf{g} \times (\mathbf{p}_{cg}^+ - \mathbf{p}) + \sum_{i \in K^+} \mathbf{f}^i \times (\mathbf{q}^i - \mathbf{p}) + \boldsymbol{\tau}^i$, where K^+ are force points on side S^+ . $\boldsymbol{\tau}^- = -\boldsymbol{\tau}^+$ by Equation 2.

To model section fracture as the breaking of a beam, we define a medial axis passing through \mathbf{p} , with direction \mathbf{v} making an equal angle to the two normals at the ends of the cross-section \mathbf{v}_1 and \mathbf{v}_2 (Figure 16c). The cross-section shape is rectangular with dimensions l and t , where l is the cross-section length projected on \mathbf{v} , and t is the thickness of the material. The section modulus (ratio of bending moment and maximum stress) for bending around \mathbf{v} is $Z_v = \frac{1}{6}t^2l$. The maximum stress for this bending direction is thus, $\sigma_v = |\boldsymbol{\tau}^+ \cdot \mathbf{v}|/Z_v$. We similarly compute bending around the normal direction \mathbf{n} of the planar section, using section modulus $Z_n = \frac{1}{6}l^2t$, and maximum bending stress $\sigma_n = |\boldsymbol{\tau}^+ \cdot \mathbf{n}|/Z_n$. Critical cross-sections have σ_v or σ_n in excess of the maximum material stress.

We performed a physical experiment (Figure 16a,b) to find that planar sections tend to fracture local to slits where sections join. We thus ensure that cross-section samples are selected aligned and local to each slit, in addition to uniformly sampling a cross-section grid over each planar section. We also note that while there is stress nonlinearity around slits, in practice we may compute a virtual stress assuming no slits and multiply it with a stress concentration factor (rarely above five). Our simulation is thus approximate but conservative, efficient and adequate for interactive modeling.

Verifying simulation predictions

We created various fabricated models that were consistent with the predictions of our physical simulation. Figure 1 shows a cutlery holder inspired by da Vinci’s “Vitruvian Man”. The two human forms were traced over the image on two orthogonal planes. The hands, contoured like the cutlery to be hung on each arm, deviated from the image. Weights were placed on the arms to simulate (viewed clockwise from

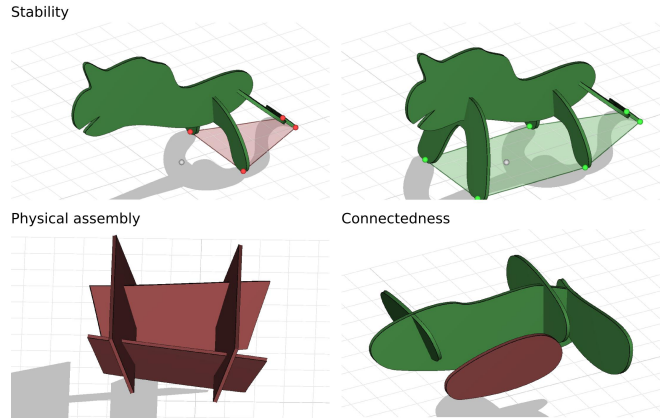


Figure 18. Our system performs various geometric feasibility tests and renders problems in red: a structure with center of mass outside the contact region will fall (top left); adding new ground contact points results in a geometrically stable model (top right); cycles of planar sections with non-parallel intersection lines cannot be physically assembled (bottom left); unconnected planar sections are flagged (bottom right).

above) 6 forks (376g), tablespoons (476g), teaspoons (185g) and knives (405g). The assembly was interactively scaled until the cutlery would hang clear of the ground, and the arms were strong enough to bear the cutlery weight. The values of the physical properties for the acrylic sheets were taken from catalogued values on a product website (density: 1190 kg/m³, tensile strength: 60 MPa).

Figure 17 shows four design variations of an object intended to hold a glass of water (275g, 350ml capacity). The first variation created had 3 thin legs, which fracture well before a glass can be filled (top row, left). Four thin legs are stronger but also fracture as predicted (top row, right). Three thicker legs just about support a full glass of water, and our system warns of a potential fracture where the legs and central disc meet (bottom row, left). A thicker 4 leg design (bottom row, right) is conservatively strong. Interactive physical feedback thus reduces wasteful real-world fabrication and testing.

FABRICATION

In addition to real-time physical simulation of the planar section structure, we perform geometric tests relating to stability, connectivity and the ability to assemble the planar sections.

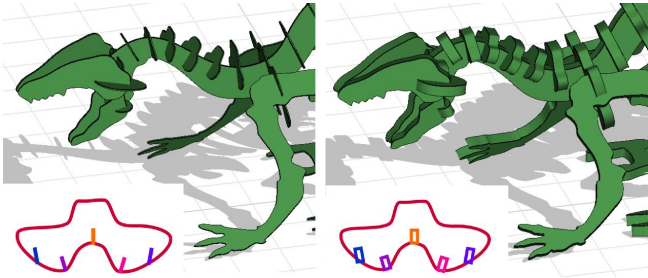


Figure 19. Adjusting planar section thickness (left: 0.02 units, right: 0.2 units). The material thickness value defines the slit width (inset).

Together, these tests ensure there are minimal issues during the fabrication process, while the model is still in digital form.

Feasibility tests

Geometric stability. Our system computes the center of mass of the model and the convex hull of any contact points with the ground plane. If the projected center of mass falls within the convex hull, the model is *geometrically stable* – it does not “fall over” when placed on a flat surface. Our system shows the convex hull of the extremal contact points and the center of mass on the ground plane (Figure 18 (top row)).

Our system also interactively translates the control points of planar section contours to remain on or above the ground plane, and visually emphasizes intersections of the current canvas plane with the ground plane. This ensures that manufactured models will have co-planar contact points.

Physical assembly. Not all planar section configurations can be physically assembled [23]. Planar sections which form cycles with non-parallel intersections make physical assembly impossible. Our system detects and reveals cycles that the user can resolve interactively (Figure 18 (bottom left)).

Connectedness. Planar sections which “float in space” cannot exist in the physical world, therefore we test *connectedness* throughout interaction. Planar sections are treated as vertices in a graph, and edges are defined by their intersections. Our system computes and reveals unconnected planar section components (Figure 18 (bottom right)).

Slits and section correspondence

Our system automatically computes the slits to cut into each planar section. For a given pair of planar sections, the axis of intersection of the planes is calculated. Then, the points on the planar section contours which intersect the axis are computed and sorted in order along the axis. When two adjacent contour points with index k and $k + 1$ along the intersection axis belong to different planar sections, an intersection condition is detected and slit rectangles are made between points p_{k+1} and p_{k+2} . To locally approximate how the two planar sections slide together, we compute and compare the distances $d_1 = \|p_k - p_{k+1}\|_2$, and $d_2 = \|p_{k+2} - p_{k+3}\|_2$. Depending on the direction, one slit endpoint will be defined by the midpoint between p_{k+1} and p_{k+2} , and the other endpoint will be either p_{k+1} or p_{k+2} .

The slits are shaped as rectangles which follow the intersection axis, with a width equal to the thickness of the planar sections as they are shown during interaction. The planar section thickness can be adjusted interactively (Figure 19). Corresponding planar section slits are assigned specific colors (or numeric labels) when output as an SVG file to aid in assembly (Figure 19 (inset)).

EVALUATION

We comprehensively evaluated our system with two groups, comprising 38 high school students and 12 users with varying artistic experience.

High School Design Class

We provided our modelling software to students taking a design class at a local high school, along lines similar to [3]. On the first day, we instructed students at a higher level for 30 minutes on how to use the software, followed by 30 minutes of working with students individually, answering questions and offering suggestions. Students in three classes, with around 15 students in each, were given a design theme: creatures, architecture, or furnishings. The students were given one week to use the software (approximately 90 minutes of use everyday). On a follow-up visit we acquired the students’ completed models (Figure 21), and had 38 students who used the software complete a questionnaire on the experience of using our software. Responses to each question were defined using a 5-point Likert scale (see Table 1).

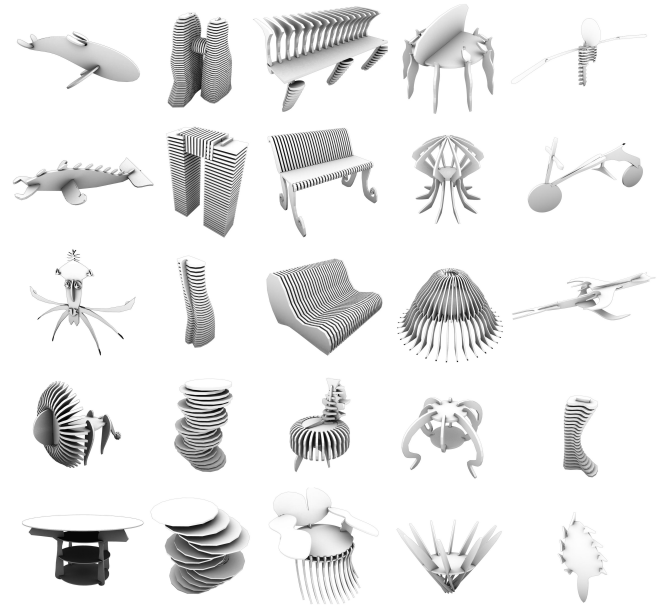


Figure 21. Models by 25 different students in a high school design class.

Other Users

We also provided our system to 12 users (with varying computer graphics experience), with a 15 minute tutorial video and a one-page instruction sheet. We show some of their creations in Figures 20 and 22. Users filled out an informal questionnaire, relating to modeling times, experience, and specific features. On average users reported: 5 to 30 minutes

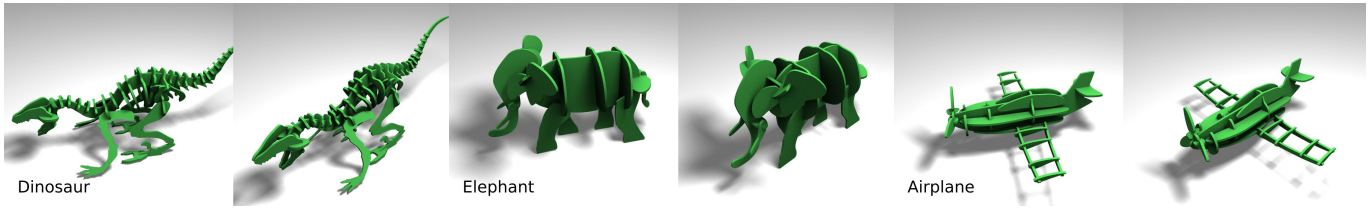


Figure 20. Planar section assemblies created using our system.

Shape modelling with planar sections?	←-----→
Creation using a single continuous stroke?	←-----→
Automatic view rotation?	←-----→
Approach to 3D view manipulation?	←-----→
The procedural modelling operations?	←-----→
Dragging control points to edit a planar section?	←-----→
Procedural modelling operations were ____ to use.	←-----→
The program was ____ to learn.	←-----→
The program was ____ to use.	←-----→
The user interface of the program was ____.	←-----→
Using the program was ____ to remember.	←-----→
I am ____ to continue using the program.	←-----→

Table 1. Evaluation by 38 high school students. Left-most values on the scale represent very negative responses and right-most values very positive responses.

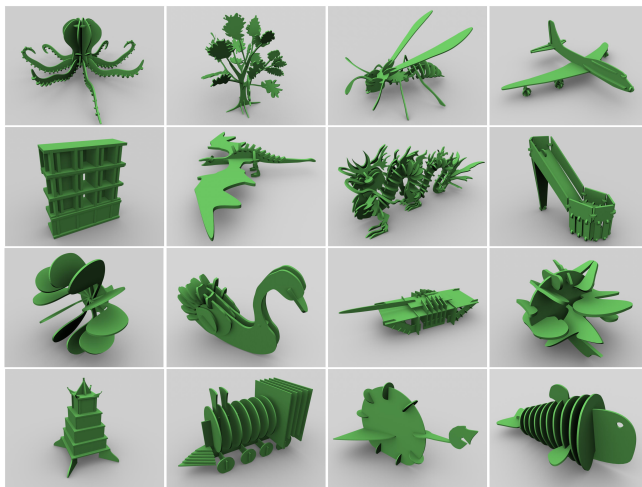


Figure 22. A gallery of creations by the 12 other users.

for system familiarity, 2 to 8 hours modeling shapes, 2 to 6 objects modeled with creation times ranging from 15 to 30 minutes. The *single stroke* interface was considered by far the most “fun” and useful feature of the interface barring one user who said he would have preferred a split-view, engineering drawing based precision workflow. The *procedural operations* were easily understood and heavily used by all users. About half the users found the *physical feedback* very meaningful. The remainder (who were not fabricating the models) did not pay any heed to it. While we support local symmetry around a slit, some users found the lack of support for global symmetry problematic and time consuming. Such a feature is easily added given our graph structure for the planar sections.

CONCLUSION

We have presented a comprehensive system for the creation of planar section assemblies with real-time geometric and physical feedback, aimed at fabricating functional objects. Various components of our drawing workflow, magnetic cuts, some procedural operations (Figure 9) and physical simulation are novel, but we believe our biggest contribution is a carefully formulated overall system design. Our system has a few missing features, such as global symmetry support or testing for global collisions when assembling sections in a given order, which are subject to future work. More exciting though, are the possibilities of transcending planar sections to assemblies composed of interlocking curved surfaces using LaserOrigami [13] or height-field sections, milled using CNC routers or 3D printers. At the same time, we expect our system to positively impact the creativity of traditional cardboard and scissor hobbyists.

Perhaps the most interesting remark from one of our set of 12 users was, “I imagine in 3D but think and draw in 2D and this system allows me to do both seamlessly, in a way I find difficult with other 3D modeling software”. We thus believe that our planar curve drawing technique will have application outside of planar section assemblies, as an overwhelming majority of 3D curves in design sketching are in fact planar [5].

REFERENCES

1. Cnc panel joinery notebook. <http://makezine.com/2012/04/13/cnc-panel-joinery-notebook/>. Accessed: 2014-07-03.
2. Bae, S., Balakrishnan, R., and Singh, K. ILoveSketch: as-natural-as-possible sketching system for creating 3d curve models. In *UIST* (2008).
3. Bae, S.-H., Balakrishnan, R., and Singh, K. Everybodylovessketch: 3d sketching for a broader audience. *UIST '09, ACM* (New York, NY, USA, 2009), 59–68.
4. Cignoni, P., Pietroni, N., Malomo, L., and Scopigno, R. Field-aligned mesh joinery. *ACM Trans. Graph.* 33, 1 (Feb. 2014), 11:1–11:12.
5. Eissen, K., and Steur, R. *Sketching: Drawing Techniques for Product Designers*. Bis Publishers, 2008.
6. Hart, G. W. Modular kirigami. *Journal of Mathematics and the Arts* (2007).
7. Hildebrand, K., Bickel, B., and Alexa, M. crdbrd : Shape Fabrication by Sliding Planar Slices. *Computer Graphics Forum (Eurographics 2012)* 31, 2 (2012).

8. Igarashi, T., Matsuoka, S., and Tanaka, H. Teddy: A sketching interface for 3d freeform design. SIGGRAPH '99, ACM Press/Addison-Wesley Publishing Co. (New York, NY, USA, 1999), 409–416.
9. Johnson, G., Gross, M., Do, E. Y.-L., and Hong, J. Sketch it, make it: sketching precise drawings for laser cutting. CHI EA '12, ACM (New York, NY, USA, 2012), 1079–1082.
10. Krecklau, L., and Kobbelt, L. Smi 2012: Full interactive modeling by procedural high-level primitives. *Comput. Graph.* 36, 5 (Aug. 2012), 376–386.
11. Li, X.-Y., Ju, T., Gu, Y., and Hu, S.-M. A geometric study of v-style pop-ups: theories and algorithms. In *SIGGRAPH* (2011), 98:1–98:10.
12. McCrae, J., Singh, K., and Mitra, N. J. Slices: a shape-proxy based on planar sections. *SIGGRAPH Asia* 30, 6 (2011), 168:1–168:12.
13. Mueller, S., Kruck, B., and Baudisch, P. Laserorigami: Laser-cutting 3d objects. In *Proceedings of the SIGCHI Conference on Human Factors in Computing Systems, CHI '13*, ACM (New York, NY, USA, 2013), 2585–2592.
14. Müller, P., Wonka, P., Haegler, S., Ulmer, A., and Van Gool, L. Procedural modeling of buildings. In *ACM SIGGRAPH 2006 Papers*, SIGGRAPH '06, ACM (New York, NY, USA, 2006), 614–623.
15. Oh, J.-H., Hanson, D., Kim, W.-S., Han, Y., Kim, J.-Y., and Park, I.-W. Design of android type humanoid robot albert hubo. In *IROS* (2006), 1428–1433.
16. OH, Y., JOHNSON, G., GROSS, M., and DO, E.-L. The designosaur and the furniture factory. In *Design Computing and Cognition 06*, J. GERO, Ed. Springer Netherlands, 2006, 123–140.
17. Paczkowski, P., Kim, M. H., Morvan, Y., Dorsey, J., Rushmeier, H., and O'Sullivan, C. Insitu: Sketching architectural designs in context. *ACM Transactions on Graphics* 30, 182 (12/2011 2011).
18. Prévost, R., Whiting, E., Lefebvre, S., and Sorkine-Hornung, O. Make It Stand: Balancing shapes for 3D fabrication. *ACM Transactions on Graphics (proceedings of ACM SIGGRAPH)* 32, 4 (2013), 81:1–81:10.
19. Rivers, A., Durand, F., and Igarashi, T. 3d modeling with silhouettes. In *ACM SIGGRAPH 2010 Papers*, SIGGRAPH '10, ACM (New York, NY, USA, 2010), 109:1–109:8.
20. Saul, G., Lau, M., Mitani, J., and Igarashi, T. Sketchchair: An all-in-one chair design system for end users. In *Tangible, Embedded, and Embodied Interaction*, TEI '11, ACM (2011), 73–80.
21. Schmidt, R., Khan, A., Kurtenbach, G., and Singh, K. On expert performance in 3D curve-drawing tasks. In *Proceedings of EUROGRAPHICS Symposium on Sketch-Based Interfaces and Modeling (SBIM)* (2009).
22. Schmidt, R., Khan, A., Singh, K., and Kurtenbach, G. Analytic drawing of 3d scaffolds. *ACM Transactions on Graphics* 28, 5 (2009), (to appear). Proceedings of SIGGRAPH ASIA 2009.
23. Schwartzburg, Y., and Pauly, M. Fabrication-aware design with intersecting planar pieces. *Computer Graphics Forum (Proceedings of Eurographics 2013)* 32, 2 (2013).
24. Shao, C., Bousseau, A., Sheffer, A., and Singh, K. Crossshade: shading concept sketches using cross-section curves. *SIGGRAPH* 31, 4 (2012), 45:1–45:11.
25. Sutherland, I. E. Sketch pad a man-machine graphical communication system. In *Proceedings of the SHARE Design Automation Workshop, DAC '64*, ACM (New York, NY, USA, 1964), 6.329–6.346.
26. Timoshenko, S. *Theory of Elasticity*, 3 ed. McGraw-Hill College, 6 1970.
27. Umetani, N., Igarashi, T., and Mitra, N. J. Guided exploration of physically valid shapes for furniture design. *ACM Trans. Graph.* 31, 4 (July 2012), 86:1–86:11.
28. Umetani, N., and Schmidt, R. Cross-sectional structural analysis for 3d printing optimization. In *SIGGRAPH Asia 2013 Technical Briefs*, SA '13, ACM (New York, NY, USA, 2013), 5:1–5:4.
29. Whiting, E., Shin, H., Wang, R., Ochsendorf, J., and Durand, F. Structural optimization of 3d masonry buildings. *ACM Transactions on Graphics* 31, 6 (2012), 159:1–159:11.
30. Willis, K. D., Lin, J., Mitani, J., and Igarashi, T. Spatial sketch: bridging between movement and fabrication. In *In Proc. Tangible, embedded, and embodied interaction* (2010), 5–12.
31. Zhu, K., and Zhao, S. Autogami: a low-cost rapid prototyping toolkit for automated movable paper craft. In *Proceedings of the SIGCHI Conference on Human Factors in Computing Systems, CHI '13*, ACM (New York, NY, USA, 2013), 661–670.